Physica C 195 (1992) 241–257
North-Holland

PHYSICA C

Optimization of depositing $Y_1Ba_2Cu_3O_{7-\delta}$ superconducting thin films by excimer laser ablation with CO_2 laser-heated substrates

K.H. Wu [a], J.Y. Juang [a], C.L. Lee [b], T.C. Lai [a], T.M. Uen [a] and Y.S. Gou [a]

[a] *Institute of Electrophysics, and*

[b] *Institute of Electro-Optical Engineering, National Chiao-Tung University, Hsinchu, Taiwan*

S.L. Tu, S.J. Yang and S.E. Hsu

Materials Research and Development Center, Chung-San Institute of Science and Technology, Longtan, Taiwan

Received 29 January 1992

The optimum deposition conditions for growing $Y_1Ba_2Cu_3O_{7-\delta}$ superconducting thin films in situ by using xenon, Nd:YAG, and KrF excimer lasers with CO_2 laser-heated substrates were studied. The dependences of the T_{c0} and microstructure of the films on the deposition parameters such as substrate temperature, oxygen partial pressure, laser energy density and repetition rates have been investigated systematically. It was found that both the surface mobility on the substrate and the reaction temperatures for the particulates arriving at the substrates are the key factors for obtaining high-quality films. High-quality $Y_1Ba_2Cu_3O_{7-\delta}$ thin films with mirror-like surface morphology, $T_{c0} \approx 90$ K, and nearly perfect *c*-axis oriented normal to the film surface were routinely grown in situ on $SrTiO_3$ substrates with the following deposition conditions: substrate temperature at 670°C, oxygen partial pressure of 0.1 torr, laser energy density of 4 J/cm^2 per pulse, and repetition rate of 10 Hz. More significantly, it took only about 3 min to grow a 0.3 μm thick film and less than 50 s to cool down the film to room temperature after deposition by the present process. Subsequent processes, such as slow cooling in oxygen atmosphere or any further heat treatments, were unnecessary for the present process. The unique advantage of the present process further offered us good opportunities to delineate the effects of each deposition parameter on the detailed film growth mechanisms without having to deal with the complications introduced by prolonged post-deposition treatments. The details of all the interesting features observed will be presented and their physical implications will be discussed.

1. Introduction

The success of producing high-quality $Y_1Ba_2Cu_3O_{7-\delta}$ (YBCO) superconducting thin films has stimulated numerous studies to understand the complicated nature of the pulsed laser deposition (PLD) processes. Two major issues one has to envisage in the understanding of this intricate process are the species and their kinetic energies contained in the laser plume and the reactions taking place at the substrates of all the arriving particulates. In the former category, it is obvious that laser parameters such as wavelength, energy density and repetition rate are the primary factors as they govern the interactions between the energetic photons and the target materials. As has been pointed out by many research groups [1–9], these factors are not only the keys to retaining the stoichiometry in both the target and the resulting films but also affect the ratio of neutral to ionic species in the plasma and the kinetic energy of the ejected species. While it is generally accepted that films are grown mainly by the neutral species (in both atomic and monoxide forms of the constituent elements) rather than the ionic ones, details of how the highly energetic particles, especially the neutral and ionized atomic species, are accelerated and how the particles in the plume interact with each other are far from conclusive [7,8]. For instance, in ref. [8], although the dissociation and the reaction path of CuO were beautifully demonstrated, the laser energy densities used (0.16–0.45 J/cm^2) were below or right at the threshold values (0.35–0.4 J/cm^2) for retaining the target stoichiometry during ablation [3,10]. Hence, the results obtained, though interesting, may

not be representative for real deposition parameters commonly used in practice.

On the other hand, parameters such as the substrate temperature and oxygen partial pressures, P_{O_2}, both during and after deposition, were also found to be crucial in determining both the crystallinity and the quality of the resultant films [10–14]. In addition to having the optimum combination of highest attainable T_c and J_c, for many application purposes growing films with a smooth surface becomes the next order of business. To this end, how to eliminate the particulate deposition and outgrowth problems commonly encountered in the explosive high deposition rate laser ablation processes is important [15]. It is therefore necessary to perform a systematic study to correlate not only the depositing sources initiated in the early stage of ablation but also the adhesion and film growth behaviors at the substrates to the quality and smoothness of the resultant films.

Recently, an in situ deposition process of producing high-quality YBCO thin films characterized by a very fast cooling rate after the completion of deposition has been developed by us [10]. The rapid cooling was realized by using a ring-shaped Pyrex tube to introduce oxygen directly onto the substrate along with a separate CO_2 laser to heat the substrate holder (a quartz plate) to avoid the possible effects of the residual heat inherent in the resistive heaters. As a result, the substrate temperature, as monitored by a thermocouple placed near it, was able to cool down to room temperature from the deposition temperature (typically around 700°C) in less than one min. As we have pointed out, the extremely high cooling rate achieved in the present process has posed a question about the actual film formation mechanism [10]. The tetragonal to orthorhombic (T–O) transition due to the fast in-diffusion of oxygen around 600°C seemed inadequate to explain the results observed. Thus, it is one of the purposes of the present study to perform a series of studies by varying both the primary and secondary deposition parameters [2] systematically to provide more detailed correlations between the film properties and deposition conditions. By doing that, it is hoped that not only the optimum deposition conditions for the technologically important PLD process can be established but, more importantly, the underlying physical mechanisms for film formation involved in the process can be delineated by such comparisons. In the following, detailed results of such systematic studies will be presented along with a discussion of their physical implications.

2. Experimental

The representative setup of the deposition system is shown schematically in fig. 1. The system mainly consists of a bell-shaped Pyrex glass chamber with dimensions about 30 cm in diameter and 30 cm in height sitting on top of a stainless flange devised with various vacuum ports and optics guiding through-

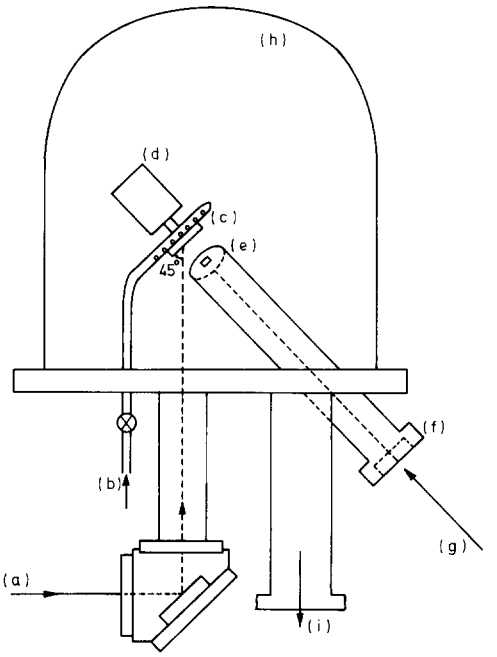

Fig. 1. A schematic diagram of the deposition setup used in this study. The target and the substrate were attached to the ends of the DC motor (d) and that of the quartz tube (e), respectively. Notice the special arrangements for the oxygen injection ring (whose position is adjustable to concentrate the O_2 streams directly onto the substrate) and CO_2 laser heating.

puts. Prior to deposition, the chamber was first evacuated to a background pressure of about 10^{-6} Torr by a mechanical pump and a turbomolecular pump (Balzers TSH240) and then back-filled to the desired P_{O_2}. The oxygen was introduced via a row of small holes ≈ 1 mm in diameter around a ring-shaped Pyrex tube, which was placed in the middle between the target and the substrate. The holes were arranged such that the oxygen streams were centered on the substrate. As has been indicated previously [10,16], such a design not only increases the cooling rate significantly, but may enhance the oxygen incorporation both during and after deposition as well.

Three laser sources were used for ablation to delineate the effects of wavelengths, pulse durations, energy densities and repetition rates. The parameters used for deposition were summarized in table 1 and their effects on the resultant films will be discussed later. For deposition, the beam was focused on the target through an anti-reflection (AR) coated window at an incident angle of 45° with respect to the normal of the target surface. The area of the elliptical spot was about 3 mm^2. The holder of the focus lens can also be translated off the optical axis to focus the spot on a different position of the target. The target was a 2 mm thick, 25 mm diameter disk of bulk YBCO prepared by typical solid-state reaction and had a T_{c0} of 88–90 K. It was rotated by a DC motor with a speed of 2500 rpm ($\approx$40 Hz) to maintain uniform ablation as well as to reduce the splashing of macroscopic particulates on the substrates [17]. Owing to the explosive nature of the ablating process, the resultant laser plume usually expands along the normal direction of the target surface. As a result, it is a common practice to place the substrates directly face-on to the target at about several centimeters distance. As will be shown below, the distance between the substrate and the target can be crucial for obtaining high-quality films. Both resistive heater (Ni–Fe–Cr wire) and CO_2 lasers were used to heat the substrates during deposition and the substrate temperatures were monitored by a thermocouple placed nearby, as has been described elsewhere [10]. Since detrimental factors, caused by severe outgassing and contaminations, were commonly encountered when the conventional heaters were used, we report only the results obtained by using a CO_2 laser to heat the substrates. The output power of the CO_2 laser was adjustable between 20–70 W with a beam diameter of about 15 mm. For the typical deposition temperature of 670°C, the output power needed was about 45 W. The typical heating-and-cooling cycle for this particular heating process is illustrated in fig. 2. It is noted that, with the use of CO_2 laser heating and the specially designed oxygen introduction arrangement, not only a stable substrate temperature can be obtained during deposition, but a very fast cooling speed can be realized. Typically, after deposition, the films can be cooled down to room temperature in less than one min which may in turn have significant implications for both superconducting phase formation mechanisms and technological applications. All the films were characterized both structurally and electromagnetically to reveal the structure–property relations. Both X-ray diffraction (XRD) and scanning electron microscopy (SEM) were used to characterize the crystallinity, orientation and surface morphology of the films obtained. The stoichiometry of the films was analyzed by energy dispersive spectroscopy (EDS) whenever necessary. For transport and magnetic properties a typical four-probe method was used. The parameters obtained from all the structure–property characterizations described above were then used to serve as the feedback for the processing parameters to further delineate their predominant effects on the PLD processes.

Table 1
The important parameters for the laser sources used in this study

Type of Laser	wavelength (nm)	peak power density (W/cm^2)	pulse duration	Repetition rate (Hz)	Y:Ba:Cu
Xe	535	10^5	30 μs	1.5	1:16:35
Nd:YAG	532	2.5×10^8	20 ns	10	1:1.8:2.9
KrF Excimer	248	5×10^8	10 ns	1–100	1:1.9:3

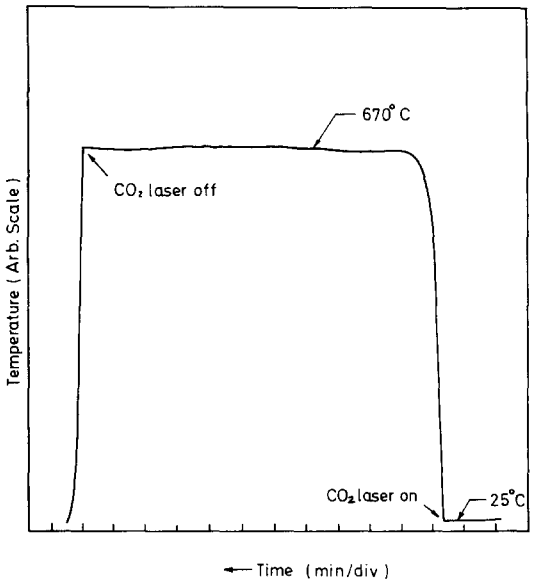

Fig. 2. The typical heating-and-cooling cycle for the present process, demonstrating the capability of maintaining stable substrate temperature during deposition and rapid cooling by using the present setup.

3. Results and discussion

3.1. Effects of the laser parameters

Figure 3 shows the typical XRD results of YBCO films using three different laser wavelengths (with other parameters held the same as described in the caption), namely 535 nm, 532 nm and 248 nm for xenon, Nd:YAG and KrF excimer lasers, respectively. The inset shows the temperature dependence of resistivities, $R(T)$, of the corresponding samples. As can be seen in fig. 3, there is no trace of superconducting phase in XRD for the film deposited by using the 535 nm xenon laser and the $R(T)$ curve exhibits typical semiconducting behavior with a negative temperature coefficient. It is noted here that the metallic atom ratios, as analyzed by EDS, for xenon laser-ablated films all showed significant deviation from the 1:2:3 stoichiometry with severe yttrium deficiency, whereas for films deposited by using other laser sources the ratios between the metallic elements were about 1:1.8:2.9 for Y:Ba:Cu. This is presumably due to the fact that, for xenon laser, neither the wavelength (i.e., photon energy) nor the peak power density (i.e., the energy density/pulse duration listed in table 1) were high enough to provide what was required for the multiphoton process and/or flash evaporation involved in the PLD processes. The fact that both the 532 nm Nd:YAG laser and the 248 nm KrF excimer laser could produce essentially the same quality of superconducting thin films further indicates that the laser wavelength might not be a critical parameter, as far as the retention of stoichiometry is concerned. As we have pointed out earlier, the effects of wavelength on the dissociation and reaction path of CuO, which may ultimately affect the oxygen content in the resultant films as demonstrated in ref. [8], were specific to the energy den-

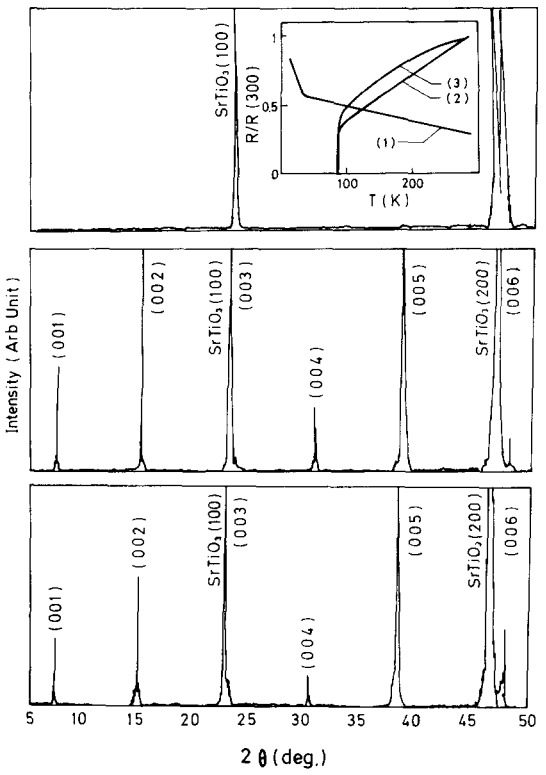

Fig. 3. The typical XRD results for the YBCO films deposited by the three different laser sources used. (Top: xenon laser; middle: KrF excimer laser; bottom: Nd:YAG laser.) The inset shows the corresponding $R(T)$ curves (curve 1: xenon; curve 2: KrF excimer laser; curve 3: Nd:YAG laser). It is evident that owing to the inadequate energy density, the superconducting phase was never obtained by using xenon laser.

sities used and may not be true in general.

On the other hand, it has been shown that the laser wavelength does affect the morphology of the film surface significantly [9]. The shorter wavelength was found to produce smoother (i.e. fewer particulates) and denser films. As shown in fig. 4, the SEM photographs taken on films made by Nd:YAG and KrF excimer lasers with comparable deposition conditions give results consistent with previous observations. The effect has been attributed to the fact that the shorter the incident laser wavelength, the smaller the absorption depth in the ceramic target and the higher the absorption by the ablated fragments, which in turn leads to smaller ablated species and further fragmentation in the hotter plume. This interpretation, however, may not represent the only solution for reducing the distribution of the particulate found in the PLD process. As pointed out by Ready [18], these particles were ejected from the target as a result of the rapid surface heating during the pulsed laser irradiation. Hence, the input energy density (a combination of the laser peak power and pulse duration) and repetition rate may also play important roles. Furthermore, it was found that the outgrowths nucleating at the triangular region formed by the coalescence of grains during the course of film growth is partly responsible for the surface roughness of the *c*-axis oriented YBCO films [14]. Thus, factors such as types of substrates used, film growth temperatures and oxygen partial pressures, which affect the film growth mechanisms to a significant extent, should all be taken into consideration in order to obtain the optimum deposition conditions for producing smooth films with best superconducting properties. In fact, in the present study, we have found that high-quality films with best surface morphologies were obtained only when operated with the optimum deposition conditions (see below).

Figure 5 shows the $R(T)$ characteristics along with the corresponding surface morphologies revealed by the SEM photographs for films deposited on (1 0 0)$SrTiO_3$ substrates with different laser pulse repetition rates. The energy density, substrate temperature and P_{O_2} used were 4.2 J/cm^2, 670°C and 0.1 Torr, respectively. Although, in fig. 5(a), we only show the representative $R(T)$ data for four repetition rates, it is noted that the T_{c0} of films deposited with a repetition rate faster than 10 Hz (up to 100 Hz) remains virtually unchanged. In contrast, significant degradation of T_{c0} and the extrapolated residual film resistance were evident when the repetition rate was reduced to 5 Hz or lower. An empirical assessment for film quality using both the linearity of $R(T)$ above T_c and the extrapolated residual resistivity indicates that the optimum repetition rate for the present study is 10 Hz. The reason for this presumably has to do with the film growth kinetics on the substrates. This is further delineated in a series of SEM results shown in fig. 5(b)–(e). At higher deposition rates, owing to the over-saturated incom-

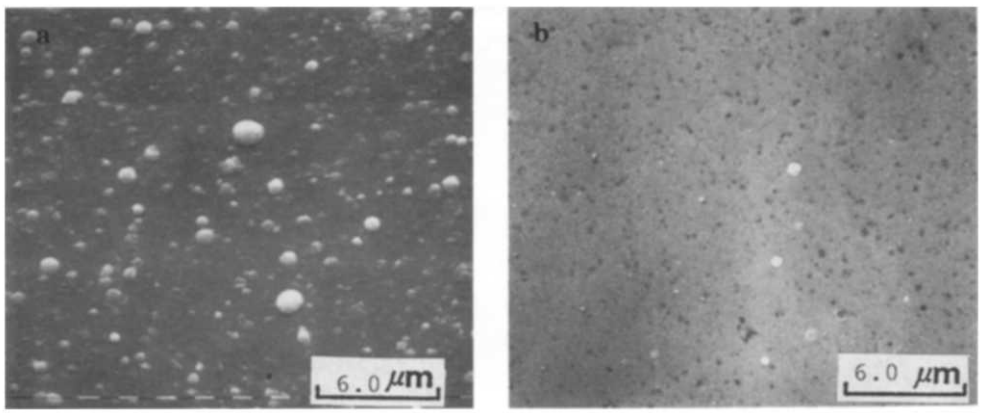

Fig. 4. SEM photographs showing the typical film surface morphology obtained by using laser sources with different wavelengths: (a) film deposited by Nd:YAG laser (532 nm), (b) film deposited by KrF excimer laser (248 nm).

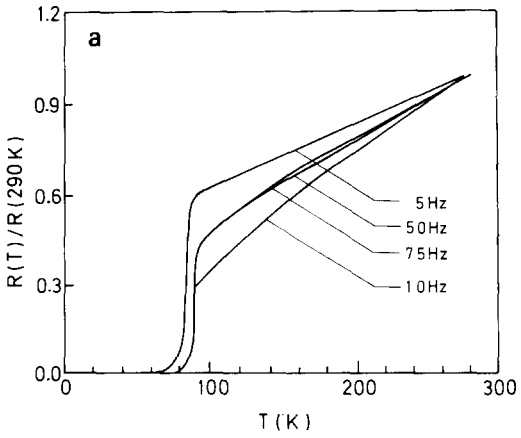

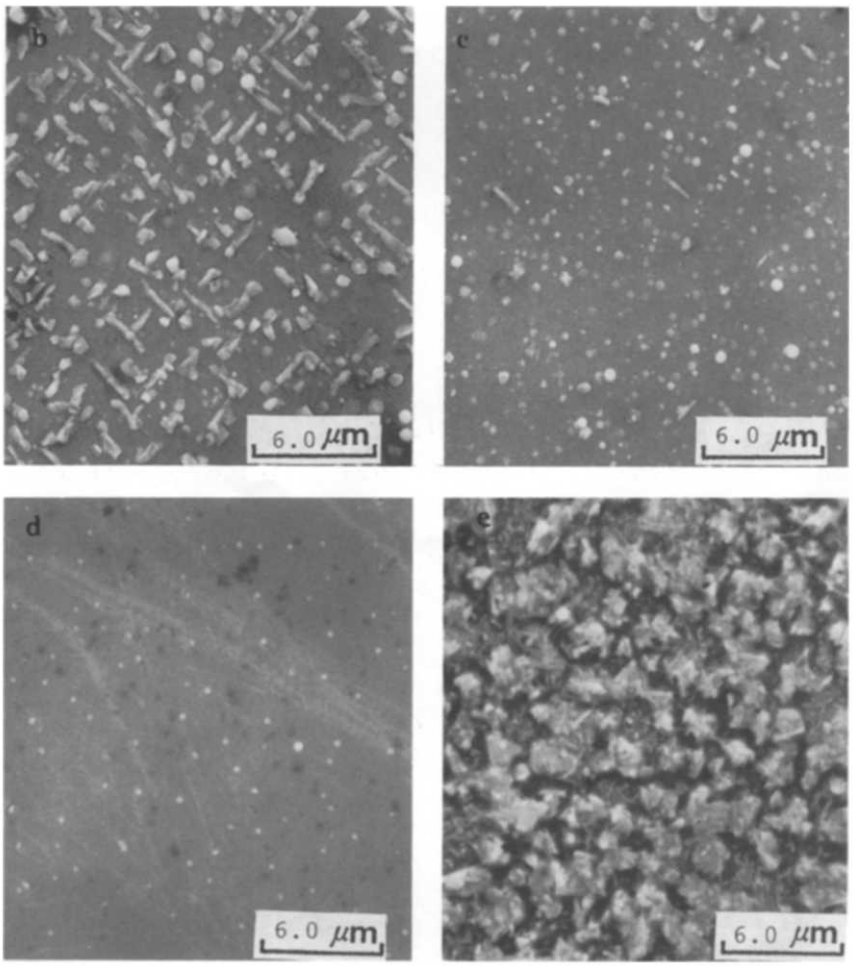

Fig. 5. (a) The representative $R(T)$ curves for films made with four different laser pulse repetition rates. (b)–(e) the corresponding film surface morphologies revealed by the SEM photographs.

ing materials, the nucleated islands coalesced at smaller thickness [15]. As a result, with a repetition rate of 75 Hz, the outgrowths (mainly *a*-axis outgrowths appearing as the orthogonal set of needles seen in fig. 5(b)) that nucleated during the grain coalescence enlarged rapidly because of their faster growth rates as compared to that of the *c*-axis [15]. In fig. 5(c), it is shown that when the repetition rate was reduced to 50 Hz, although some of these needle-shaped outgrowths are still observable, the amount has been reduced significantly and they exist only as a minor phase. As the optimum deposition rate (10 Hz here) was approached, it is clear from fig. 5(d) that the outgrowths were completely eliminated and the film is completely *c*-axis oriented with minor distribution of particulates, which in turn results in high-quality superconducting films with a very smooth surface. As has been pointed out by Chang et al. [15], the outgrowths depend strongly on the film growth mechanisms and occur favorably in cases of nucleation and growth of islands, where the intersections of the coalesced grains act as the nucleation sites of second phases which in turn provoke *a*-axis outgrowths. It is thus expected that in layer-by-layer growth situations the outgrowths should be able to be eliminated, in principle, although factors such as lattice matching and interface reaction may further complicate the simple argument offered.

For even lower deposition rates, severe degradation of film properties and surface morphologies occurred (as is evident from fig. 5(a) and (e)) owing to the prolonged deposition. For films deposited with a 5 Hz repetition rate, it typically took more than 20 min to produce a 450 nm thick film. The prolonged deposition time increases not only the opportunity for impurity adhesion but also film/substrate interactions. Furthermore, the incomplete coalescence of growing islands may also be responsible for the rough surface appearance seen in fig. 5(e). The EDS analyses over the entire film surface showed that both stoichiometry inhomogeneities and local Ba-segregations were present.

The third laser parameter investigated was the effect of laser energy density. Owing to the wider tunable range available, we report here only the results obtained by the KrF excimer laser. Figure 6(a) shows the $R(T)$ behaviors of several films deposited with different laser energy densities while other parameters were kept at their optimum values. From the results, it is clear that the effects of the laser energy density on the resulting film properties were not as dramatic as the previous ones. The slight decrease in T_{c0} of lower energy densities (see the inset of fig. 6(a)) was attributed to the increasing amount of Y_2O_3, as indicated in fig. 6(b). The existence of the Y_2O_3 is believed to result from the modification of the target surface due to the erosive nature of the ablation process, which in turn results in an Y-rich shell surrounding the core of the columns formed [20]. In any case, the minute effect of the laser energy density seems surprising and may require further investigation. Intuitively, one would expect that the higher the energy density incident on the target surface, the higher the resulting temperature leading to the production of ablated species with higher kinetic energies. This would in turn alter the deposition process to some sizable extent. The same reasoning applies even for the exotic acceleration mechanisms such as plasma potential acceleration, inverse bremsstrahlung induced high-pressure gaseous expansion, and/or self-consistent electrical field established by the rapid expansion of the ablated plume, proposed for the extraordinarily high kinetic energies of the neutral and ionic species observed by laser-induced-fluorescence and other spectroscopic measurements [7,8,21]. In that the superthermal nature of the ablated species is expected to relate to the high temperature ($\approx 10^4$ K) attained near the target surface [3,22], it should be affected by the input energy density. Another aspect of the energy density effects was the amount of material ablated per pulse [23]. Although this may not directly affect the dynamic properties of constituents contained in the plume and hence the initial stage of the film growth, nevertheless, it may change the coverage of the incoming materials on the substrate and alter the subsequent growth mechanism, as has been observed by Norton and Carter [2] in a YBCO-on-MgO system. We suspect that a similar effect may occur in the present case and partly account for the slight variations of both the superconducting properties and film crystallinity observed in fig. 6.

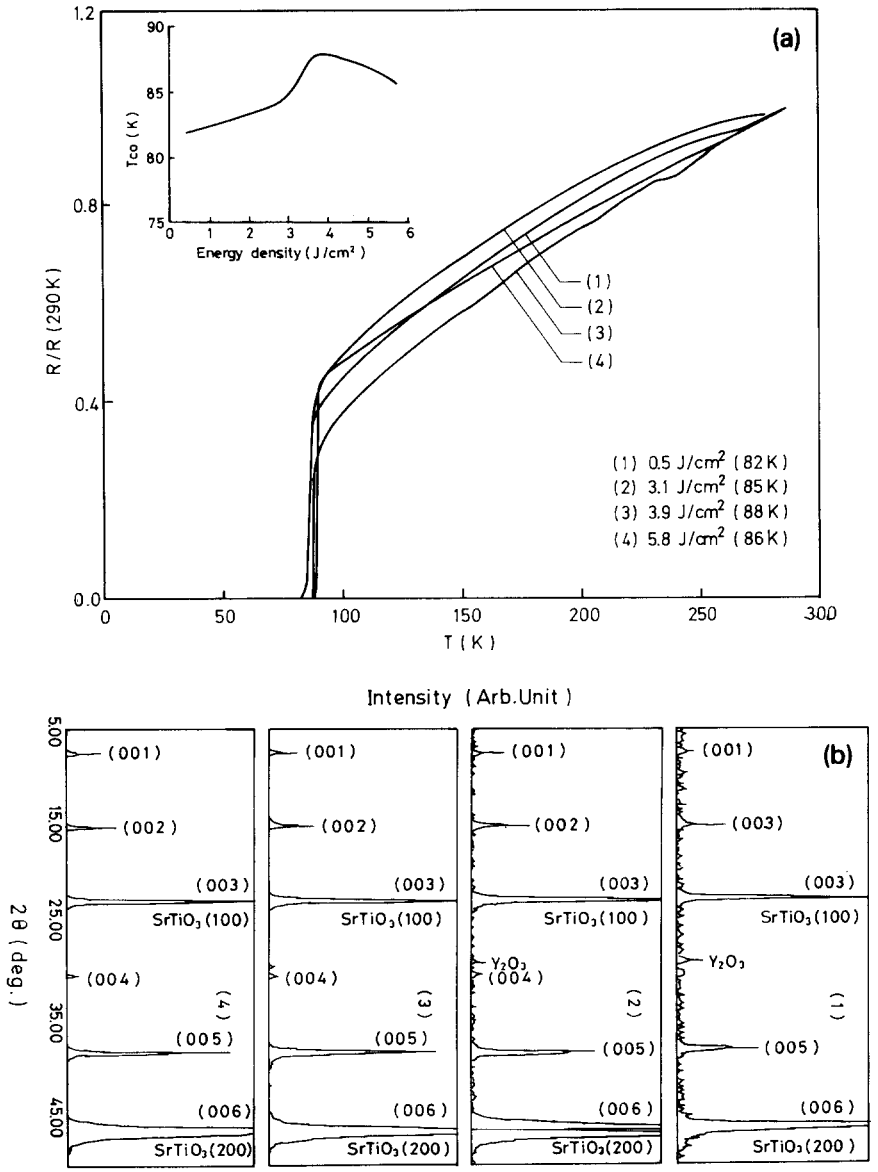

Fig. 6. (a) The $R(T)$ characteristics for films made with different laser energy densities. Numbers shown in parentheses are T_{co}s. (b) The corresponding XRD results for films shown in (a). It is interesting to note hat, except for the amount of Y_2O_3, only slight effects were observed over the wide range of energy density used.

3.2. Effects of substrate temperatures and orientations

The effects of substrate materials and orientations, as well as the temperatures at which the films were deposited, on laser-deposited superconducting thin films have been studied extensively [1–10]. It is generally accepted that both the film growth orientation and optimum growth temperature can vary significantly with the substrate materials. In this section we hope to demonstrate in a systematic manner how the substrate parameters affects the film growth

mechanisms and by what factors these influences actually take place.

In fig. 7(a–c) we show the result of transport properties, crystallinity (by XRD) and surface morphology (by SEM), respectively, for films deposited on (1 0 0)$SrTiO_3$ at various substrate temperatures. It is clear that, in terms of the three quality-evaluation parameters shown, the best quality films exist only within a very narrow window of temperatures, namely between 650°C and 700°C. It is noted that the optimum temperatures for deposition may vary with the substrate materials used [10]. In general, the predominant effects of the substrate temperature are two-fold, that is, both kinetic and chemical. By the former it determines the surface mobility of the arriving constituents, whereas by the latter it affects the prevalence of the reactions between the constituents. Both effects together determine the growth mechanism of the films. From fig. 7(c) it is seen that at 750°C, in addition to the usual distribution of particulates, there exists a significant amount of reaction products with unidentified composition on the surface of the film. This not only results in reduction of T_c but degrades the homogeneity of the films (that is, exhibits a wider ΔT_c as shown in fig. 7(a)). As the temperature decreases, it is evident that the growth behaviors of the films show a clear tendency from fast growing (manifested as incomplete grain coalescence and hence rougher surface at 700°C) to near epitaxial *c*-axis oriented films. Further decrease in substrate temperature results in incomplete reaction and hence even poorer quality films. It is also interesting to note that the substrate temperature shows virtually no effect on the particulate distributions, indicating that these massive low mobility particles probably did not participate in the film growing process. Thus, their existence may just be destroying the smoothness of the film surface and have limited influence on the intrinsic properties, such as the film stoichiometry and crystallographic orientation, etc. To eliminate or to reduce the size of these particulates one may have to modify the laser parameters, as has been discussed in previous paragraphs.

The effects of substrate materials and their crystallographic orientation on the film deposition were also investigated. Both the shift of optimum deposition temperature window and variations in film

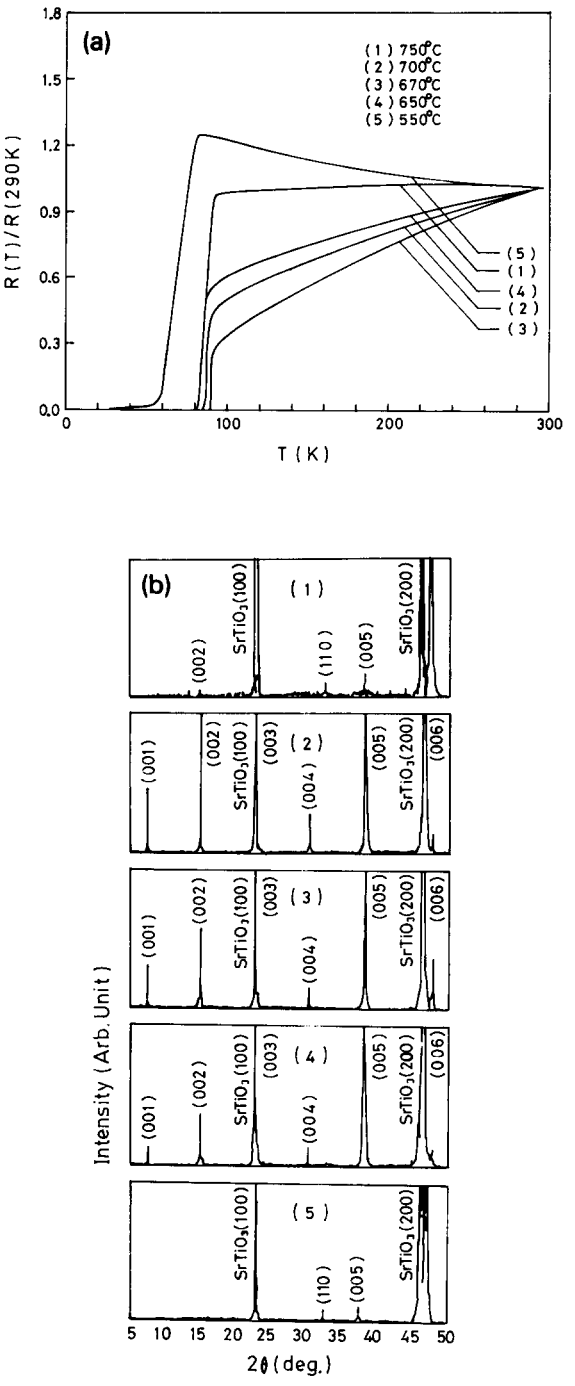

Fig. 7. The film quality as a function of substrate temperatures delineated by: (a) transport $R(T)$ characteristics, (b) crystallinity (XRD), and (c) surface morphologies (SEM) results for films deposited on (1 0 0)$SrTiO_3$ substrates.

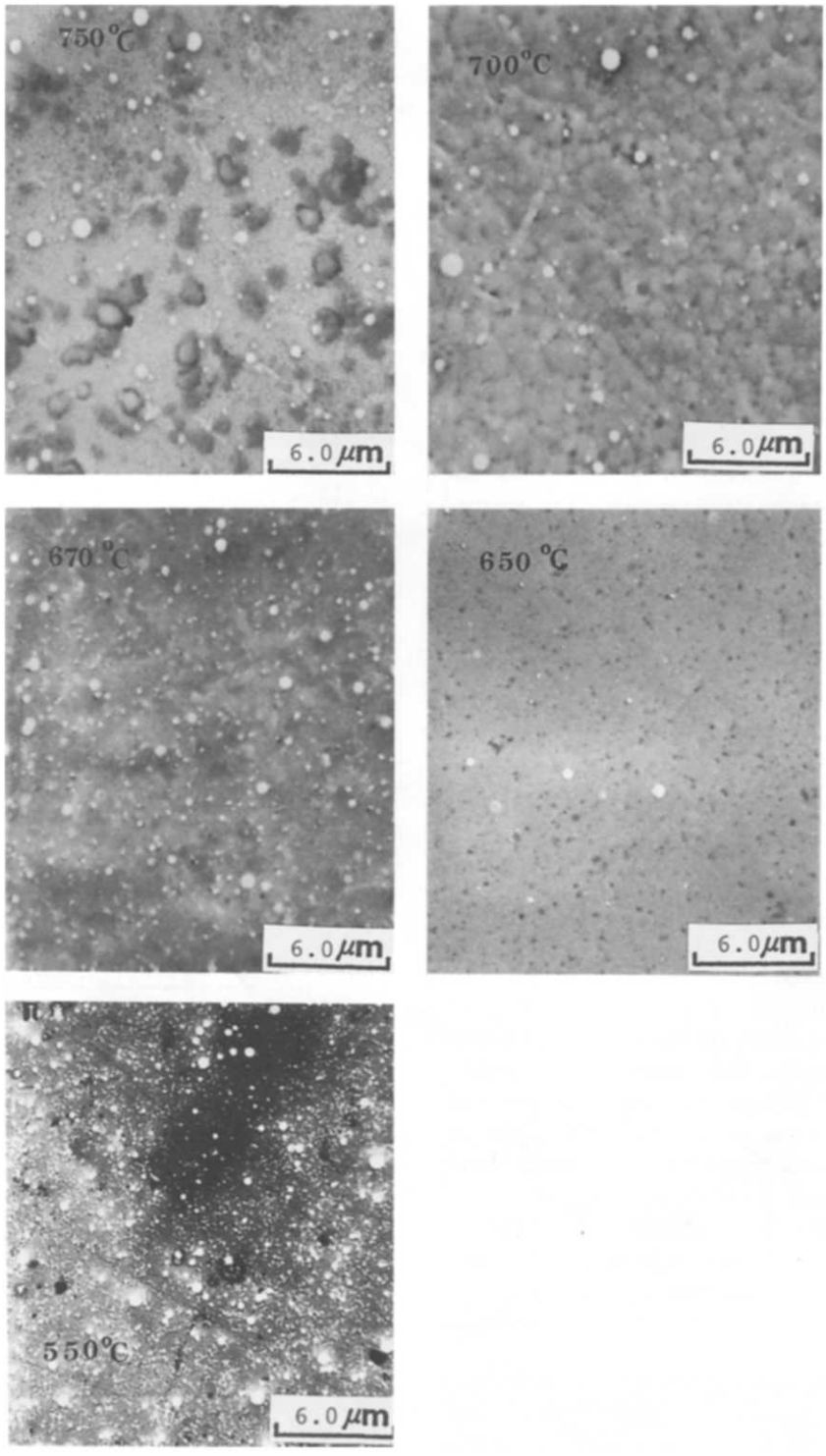

Fig. 7. Continued.

texturing orientations were observed. The effects were believed to be mostly due to the epitaxial nature of the film growth mechanism [24]. Each substrate and its respective orientation provides a set of lattice matching conditions combined with the favorable kinetics for a particular crystallographic orientation of YBCO films to grow epitaxially. The versatility of choices has opened up good opportunities for making high-quality films with various orientations in a well-controlled manner. As an example, in fig. 8 the representative result of a high-quality, pure, (1 1 0)-oriented YBCO film deposited on a (1 1 0)$SrTiO_3$ substrate with compatible deposition conditions is shown. It is encouraging to note that not only good transport properties but clean film crystallinity can be achieved by the present process, as was evident from both the $R(T)$ characteristic (fig. 8(a)) and the XRD result (fig. 8(b)). This further suggests that it should be possible to fabricate sharply controlled misoriented films in situ by using an angle-cut substrate during the same deposition run. We are currently exploring the feasibility of this idea to make films that may have significance for both device applications and fundamental studies in anisotropic flux line dynamics.

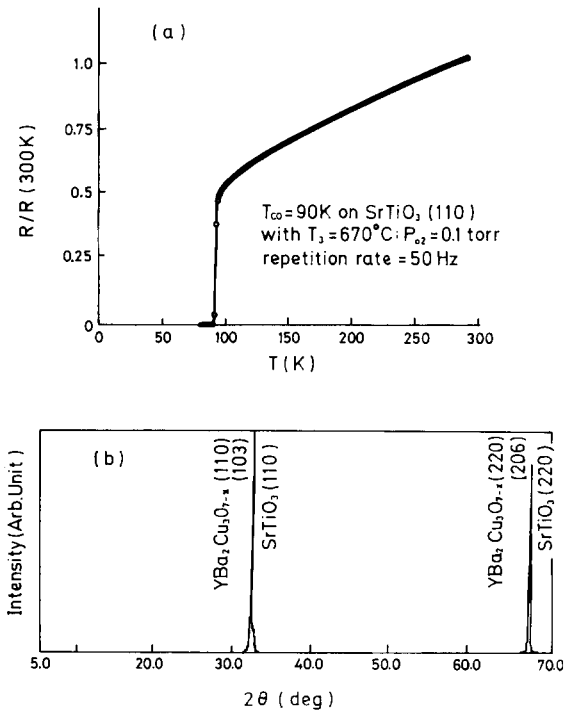

Fig. 8. (a) The typical $R(T)$ result for high-quality (1 0 0)-YBCO films deposited on (1 1 0)$SrTiO_3$ substrate. (b) The XRD result for the corresponding film, indicating the clean (1 1 0) texturing of this film.

3.3. Effects of oxygen streams

Unlike other HTSC systems, the YBCO phase is a line-compound and hence its superconducting properties are very sensitive to the oxygen stoichiometry [25]. As a result, in order to obtain films with best superconductivities in situ, it is very important to incorporate the right amount of oxygen into the films during various stages of deposition. Methods such as introducing activated oxygen species by using RF-induced plasma [26] or photoionization induced by the ablating laser beam [27] during deposition and prolonged annealing at around 450°C in ambient P_{O_2} after the completion of deposition [2–9,25–27] were practiced with impressive successes. However, as we have pointed out previously [10], the role of P_{O_2} in both oxygen incorporation and film growth mechanisms during the deposition process was hidden to some extent owing to the slow cooling required in most early reports to obtain superconductivity [2–9,11–13,25–29]. Issues such as whether the superconducting orthorhombic phase can be formed in situ during deposition to avoid the tetragonal–orthorhombic phase transition at around 500°C during cooling, which could be detrimental to film properties owing to the large accompanying stress, and how the P_{O_2} affects the oxygen stoichiometry and film growth mechanisms both during and after deposition, remained to be clarified. With the specific oxygen stream injection arrangements used in the present study (see fig. 1), it was demonstrated [10] that high-quality superconducting films could be obtained in situ without slow cooling. The elimination of the effects resulting from slow cooling has made it possible to study the issues outlined above. We report here the detailed results observed by varying P_{O_2} and in situ measuring of film resistances to delineate both the film growth mechanisms and oxygen incorporation processes during deposition.

Figure 9(a–f) shows the XRD pattern and surface

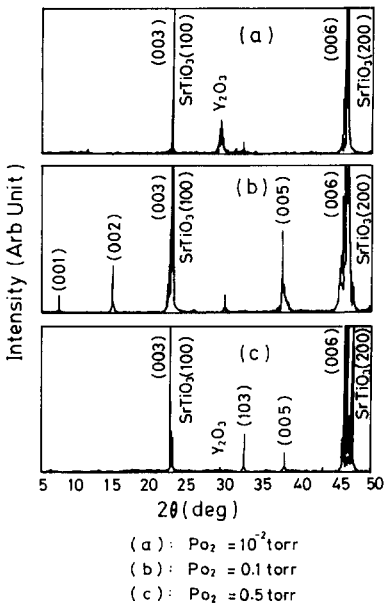

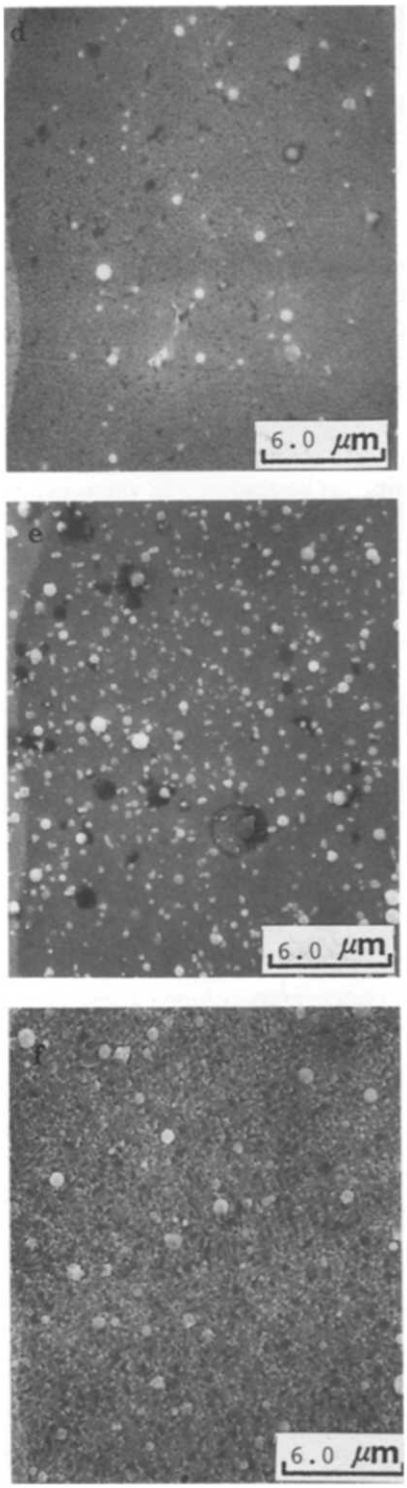

Fig. 9. (a–c) the XRD results for films deposited at different oxygen partial pressures, indicating the significant effects of P_{O_2} on both the growth behavior and film quality. (d–f) The SEM photographs showing the film surface morphologies for the corresponding films shown in (a–c).

morphologies for films deposited as a function of P_{O_2}. As can be seen in fig. 9(a–c), the crystallinity of the films depends strongly upon the P_{O_2} used during deposition. At both high (greater than 0.5 Torr) and low (say 10 mTorr or less) P_{O_2}, not only a significant amount of second phase (Y_2O_3) was present but a noticeable extent of (1 0 3) outgrowths was evident. The corresponding film morphologies for fig. 9(a–c) are displayed by the SEM photographs shown in fig. 9(d–f), respectively. The evolution of (1 0 3) outgrowths at higher P_{O_2} was clearly seen [24]. In the present study, the optimum P_{O_2} during deposition was found to be located in the vicinity of 0.1–0.2 Torr. These results differed somewhat from the results reported by Hase et al. [12], in that a much lower optimum P_{O_2} (in the range of 10–50 mTorr) was reported. We note here that, owing to the special arrangement of the present system, the actual P_{O_2} right around the substrate can be even higher than the average chamber pressure. Although the discrepancies found here may arise partly from the detailed design of the systems used, it is believed, physically, to result mainly from the interactions between the laser plume and the oxygen streams. For instance, it has been pointed out by Kwok et al. [29] that the optimum P_{O_2} for depositing YBCO films by using an ArF excimer laser ($\lambda = 193$ nm) was 10–50 mTorr, whereas it changed to 0.1–0.2 Torr when a KrF excimer laser ($\lambda = 248$ nm) was used. In the present case, the oxygen was introduced right on the substrate instead of near the target or by simply filling the chamber, and thus the recombination of activated oxygen species excited by the energetic constituents contained in the laser plume due to Rayleigh scattering was minimized. As a result, not only did the laser plume reach the substrate in a uniform manner but the oxygen activated near the substrate could incorporate into the film formation directly to promote the stoichiometry of the resulting phase (see below). We have evidently found that the distances between the target and substrate (from 4 to 7.5 cm) did not influence the deposition results noticeably. Nevertheless, for distances shorter than 4 cm, the resulting films were degraded somewhat, which was presumably due to the resputtering effects.

To further delineate how the P_{O_2} influences the film growth behaviors, we have monitored it by in situ resistance measurements following the method suggested by Ying et al. [28]. Figure 10 summarizes several typical features observed in such a study. The results are for films deposited at $T_s = 670\,^{\circ}C$, $P_{O_2} = 0.1$ Torr and a repetition rate of 50 Hz. Curve (2) in fig. 10 shows the typical behavior of time- (or equivalently thickness-) dependent resistance for films deposited on YSZ substrates. The initial drop in resistance at the beginning of deposition is similar to that reported by Ying et al. [28] and was attributed to a continuous layer of orthorhombic phase formation as delineated by in situ XRD studies. This orthorhombic layer was then degraded by the formation of interface compound or nonsuperconducting tetragonal phase because of oxygen out-diffusion [28,29] as the deposition proceeds. However, in our case, the resistance gradually decreases with further deposition instead of increasing or staying at a constant resistance as reported by Ying et al. [28], indicating that, owing to the difference in P_{O_2} used, the film growth mechanism may have been altered. For instance, the initially tightly formed boundary layer may be followed by nucleation and growth mechanism due to the formation of interface compounds [30]. We have checked the effects of changing P_{O_2} within the range of 0.1 to 1 Torr on this particular behavior and virtually similar results were observed. Since at temperatures above 500 °C the oxygen content in the YBCO films has been found to be essentially in thermal equilibrium with P_{O_2} and is very oxygen deficient [13,29], the present results cannot be explained by the changes in oxygen content only. Alternatively, this may result from the reduction of grain boundary area, due to continuous grain growth during the course of deposition, combined with better oxygen incorporation to further reduce the resistivity of the grain boundaries. As can be seen in fig. 11(a), the final grain structure for films deposited on YSZ shows a typical morphology of grain coalescence [15] with large copper oxides (see the EDS comparisons for different regions shown in figs. 11(b) and (c)) nucleated at the triangular intersects between coalesced grains. This further indicates that the original layer growth mechanism was altered during deposition as suggested above and lends a piece of strong evidence supporting our view of grain boundary effects on the film resistance change described above.

In contrast to that described above for YSZ sub-

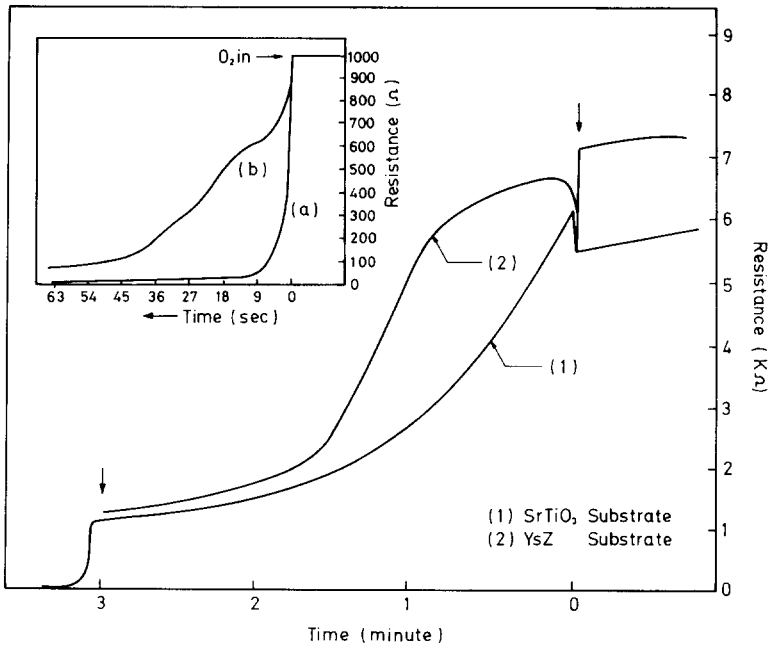

Fig. 10. The results of in situ resistance measurements for films deposited on different substrates with exactly the same deposition parameters, indicating the evolution of the film growth mechanisms. The inset shows the effect of cooling rates (or equivalently the oxygen partial pressures) on the in situ film resistance changes for films deposited on (1 0 0)$SrTiO_3$ substrates after the completion of deposition, indicating the quickness of oxygen incorporation and its effect on the resultant films. Curve (a) in the inset is the result for fast cooling and curve (b) is that for slow cooling (i.e. the oxygen flows in slowly).

strates, curve (1) in fig. 10 shows the typical behavior manifested by films deposited on (1 0 0)$SrTiO_3$ substrates with the same deposition conditions. As can be seen, the resistance increases instantly as the deposition commences then decreases continuously as the deposition proceeds. The dramatic differences observed at the very early stage of deposition suggest that the nucleation and growth mechanism was quite different in the two cases. For $SrTiO_3$ it is suggestive that discrete islands were formed instead of a continuous layer followed by nucleation and growth as found in YSZ. In any case, as suggested by the similar general trends in decreasing film resistances, the detailed grain coalescence process was believed to be responsible for the results observed. The fact that about the same value of the film resistances was found in both cases further suggests that similar materials were growing. That the final magnitude of film resistance reaches a value of about 1 kΩ($\approx$0.05 Ω cm for a typical film thickness of 500 nm) in both cases indicates that either very oxygen-deficient tetragonal phases were formed [31] or highly resistive grain boundaries were dominating the overall film resistance at the completion of deposition.

In the inset of fig. 10, the subsequent film resistance changes as a function of cooling rates were compared. The cooling rate was controlled by the speed of oxygen introduction with the heating laser off in both cases. For fast cooling (curve (a)) the chamber was filled with about 1 atm of oxygen in less than 5 s immediately after the completion of deposition. As can be seen, in this case, the film resistance shows an abrupt drop in the first 10 s then saturates at a final value of a few tens of Ω, indicating that a good superconducting orthorhombic phase was formed [31]. If one compares this with the corresponding temperatures (as shown in fig. 2), it suggests that a diffusivity as large as 10^{-10} cm^2/s is required for the T–O transition to prevail with correct oxygen stoichiometry. Although such a high diffusion coefficient has been routinely used to interpret

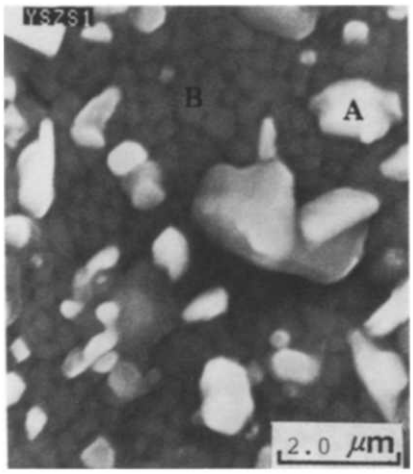

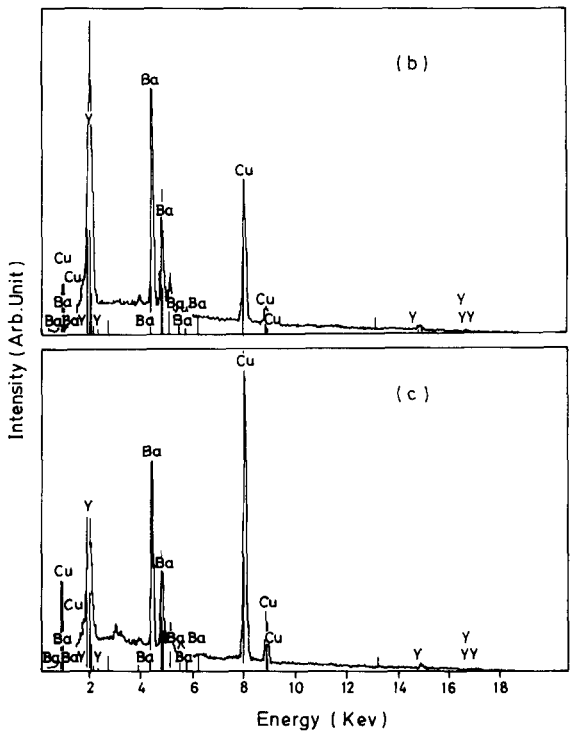

Fig. 11. (a) The typical SEM result for films deposited on (1 0 0) YSZ substrates. (b) The EDS result for area B marked in (a), showing the typical stoichiometric YBCO spectrum. (c) The EDS spectrum for area A marked in (a). The much higher relative intensity for Cu is evident.

the experimental results obtained by many groups [13,28,29] and represents the core assumption for the above-mentioned superconducting phase formation mechanism, the physical validity of it remains to be justified. In a recent study of oxygen tracer diffusion in YBCO, Rothman et al. [32] have shown that the diffusion of oxygen is very anisotropic and insensitive to P_{O_2} with $D_b \approx 10 D_{ab}$ ($\approx D_{poly}$) $\approx 10^4$–$10^6 D_c$ and $D_b \approx 10^{-12}$ cm^2/s in the temperature range considered here, where D_b, D_{ab}, D_{poly} and D_c are the diffusivities along the b-axis, in the ab-plane, in polycrystals and along the c-axis, respectively. As can be seen, the diffusivity required for the fast oxygen uptake-induced T–O transition mechanism was two orders of magnitude larger than even the fastest b-axis diffusion considered. As a result, it appears that the oxygen incorporation in the final stage of the film formation process requires further systematical studies to give a quantitative account of the accumulated observed results. Since the large diffusivity obtained can be rationalized only by taking the grain boundary diffusion as the major diffusion path, we suggest that the final stage of oxygen incorporation must have modified the grain boundary structure as well, rather than having induced intragranular phase transition only. This alternative explanation also provides a more consistent physical picture with the in situ film resistance changes discussed above.

In contrast to that, in the slow cooling case where the oxygen was introduced gradually with a speed of 10 Torr/s, the film resistance shows a rather complicated behavior as a function of time (or equivalently P_{O_2}), as shown by curve (b) in the inset of fig. 10. We suspect that the initial drop in film resistance reflects the initially fast oxygen diffusion at higher temperatures; however, owing to the decrease in temperature and smaller P_{O_2}, the oxygen uptake is sluggish and incomplete, resulting in very defective intragranular phase and grain boundaries. Evidently, films subject to the slow cooling process all showed higher final resistance and severe degradation in T_c. In general, T_cs dropped from typically around 90 K (as obtained by fast cooling) to about 40 K with very wide transitions. All these results suggest that, after deposition, the phase transition (if it does occur), as well as the correct oxygen stoichiometry, was accomplished within 10 s provided the environment P_{O_2}

was high enough. The slow cooling and prolonged annealing around 400–500°C required in earlier reports [1–9,11–29] turned out to have only little effect on the resultant films.

4. Summary

The dependences of the T_{c0} as well as the crystallinities and surface morphologies of the films on the deposition parameters such as substrate temperature, oxygen partial pressure, laser energy density and repetition rates in in situ grown YBCO superconducting thin films using a KrF excimer laser with CO_2 laser-heated substrates have been investigated systematically. It was found that both the surface mobility on the substrate and the reaction temperatures for the particulates arriving at the substrates are the key factors for obtaining high-quality films. High quality $Y_1Ba_2Cu_3O_{7-\delta}$ thin films with mirror-like surface morphology, $T_{c0} \approx 90$ K, and nearly perfect *c*-axis orientation normal to the film surface were routinely grown in situ on $SrTiO_3$ substrates with the following deposition conditions: substrate temperature at 670°C, oxygen partial pressure of 0.1 Torr, laser energy density of 4 J/cm^2 per pulse, and repetition rate of 10 Hz. It was found that essentially the same deposition conditions applied equally well to $\langle 110 \rangle$ oriented films deposited on (1 1 0)$SrTiO_3$ substrates. This suggests that, in addition to the substrate temperature and oxygen partial pressure, the substrate orientation may also play an important role in determining the orientation of the resultant films. The unique advantage of the fast cooling capability realized in the present process has offered opportunities, for the first time, to delineate the effects of each deposition parameter in a more straightforward manner by eliminating the complications introduced by prolonged post-deposition treatments.

Acknowledgements

We are indebted to Prof. H.S. Kwok for many useful discussions during the course of this study. This work was supported in part by the National Science Council, Taiwan, under grant Nos. NSC-81-0208-M009-501 and NSC81-0208-M009-28.

References

[1] R.K. Singh and J. Narayan, Phys. Rev. B 41 (1990) 8843.
[2] M.G. Norton and C.B. Carter, Physica C 172 (1990) 47.
[3] P.E. Dyer, R.D. Greenough, A. Issa and P.H. Key, Appl. Phys. Lett. 53 (1988) 534.
[4] X.D. Wu, B. Dutta, M.S. Hedge, A. Inam, T. Venkatesan, E.W. Chase, C.C. Chang and R. Howard, Appl. Phys. Lett. 54 (1989) 179.
[5] O. Auciello, S. Athavale, O.E. Hankins, M. Sito, A.F. Schreiner and N. Biunno, Appl. Phys. Lett. 53 (1988) 72.
[6] O. Eryu, K. Murakami, K. Masuda, A. Kasuya and Y. Nishina, Appl. Phys. Lett. 54 (1989) 2716.
[7] H. Izumi, K. Ohata, T. Sawada, T. Morishita and S. Tanaka, Appl. Phys. Lett. 59 (1991) 597.
[8] C.E. Otis and R.W. Dreyfus, Phys. Rev. Lett. 67 (1991) 2102.
[9] G. Koren, A. Gupta, R.J. Baseman, M.I. Lutwyche and R.B. Laibowitz, Appl. Phys. Lett. 55 (1989) 2450.
[10] K.H. Wu, C.L. Lee, J.Y. Juang, T.M. Uen and Y.S. Gou, Appl. Phys. Lett. 58 (1991) 1089.
[11] M. Ohbuko, T. Kachi, T. Hioki and J. Kawamoto, Appl. Phys. Lett. 55 (1989) 899.
[12] T. Hase, H. Izumi, K. Ohata, K. Suzuki, T. Morishita and S. Tanaka, J. Appl. Phys. 68 (1990) 374.
[13] M. Ohbuko, T. Kachi and T. Hoiki, J. Appl. Phys. 68 (1990) 1782.
[14] G. Koren, A. Gupta and R.J. Baseman, Appl. Phys. Lett. 54 (1989) 1920.
[15] C.C. Chang, X.D. Wu, R. Ramesh, X.X. Xi, T.S. Ravi, T. Venkatesan, D.M. Huang, R.E. Muenchausen, S. Foltyn and N.S. Nogar, Appl. Phys. Lett. 57 (1990) 1814.
[16] R.K. Singh, L. Ganapathi, P. Tiwari and J. Narayan, Appl. Phys. Lett. 55 (1989) 2351.
[17] J.T. Cheung and H. Sankur, CRC Crit. Rev. on Solid State Mater. Sci. 15 (1988) 63.
[18] J.F. Ready, Effects of High Power Laser Radiation (Academic Press, New York, 1971).
[19] R. Ramesh, T.S. Ravi, D.M. Huang, C.C. Chang, A. Inam, T. Venkatesan, X.D. Wu, R.E. Muenchausen, S. Foltyn and N.S. Nogar, Physica C 173 (1991) 163.
[20] S.R. Foltyn, R.C. Dye, K.C. Ott, E. Peterson, K.M. Hubbard, W. Hutchinson, R.E. Muenchausen, R.C. Estler and X.D. Wu, Appl. Phys. Lett. 59 (1991) 594.
[21] A.V. Gurvich, L.V. Pariiskaya and L.P. Pitaevskii, Sov. Phys. JETP 36 (1973) 274.
[22] A. Inam, X.D. Wu, T. Venkatesan, S.B. Ogale, C.C. Chang and D. Dijkkamp, Appl. Phys. Lett. 51 (1987) 1112.
[23] R.K. Singh, O.W. Holland and J. Narayan, J. Appl. Phys. 68 (1990) 233.

[24] C.B. Eom, J.Z. Sun, B.M. Lairson, S.K. Streiffer, A.F. Marshall, K. Yamamoto, S.M. Anlage, J.C. Bravman, T.H. Geballe, S.S. Laderman, R.C. Taber and R.D. Jacowitz, Physica C 171 (1990) 354.
[25] R.J. Cava, B. Batlogg, C.H. Chen, E.A. Rietman, S.M. Zahurak and D. Werder, Nature 329 (1989) 423.
[26] S. Witanachchi, H.S. Kwok, X.W. Wang and D.T. Shaw, Appl. Phys. Lett. 53 (1988) 234.
[27] J.P. Zheng, Q.Y. Ying, S. Witanachchi, Z.Q. Huang, D.T. Shaw and H.S. Kwok, Appl. Phys. Lett. 54 (1989) 954.
[28] Q.Y. Ying, H.S. Kim, D.T. Shaw and H.S. Kwok, Appl. Phys. Lett. 55 (1989) 1041.
[29] H.S. Kwok and Q.Y. Ying, Physica C 177 (1991) 122; H.S. Kwok, private communications.
[30] See for example, M.J. Stowell, in: Epitaxial Growth, ed. J.W. Matthews (Academic Press, N.Y., 1975) p. 437.
[31] P.P. Freitas and T.S. Plaskett, Phys. Rev. B 36 (1987) 5723.
[32] S.J. Rothman, J.L. Routbort, U. Welp and J.E. Baker, Phys. Rev. B 44 (1991) 2326.